

See discussions, stats, and author profiles for this publication at: <https://www.researchgate.net/publication/315349402>

## Overview and status of construction of ST40

**Article** in Fusion Engineering and Design · March 2017

DOI: 10.1016/j.fusengdes.2017.03.011

---

CITATIONS

2

READS

51

### 2 authors:



**Mikhail Gryaznevich**

Tokamak Energy Ltd

**78** PUBLICATIONS **350** CITATIONS

SEE PROFILE



**Otto Asunta**

Aalto University

**52** PUBLICATIONS **409** CITATIONS

SEE PROFILE

### Some of the authors of this publication are also working on these related projects:



Simulations of confinement for ST40 high field Spherical Tokamak [View project](#)



Effects of 3D geometry ferromagnet materials on magnetic fields in their vicinity [View project](#)

# Overview and status of construction of ST40

M. Gryaznevich<sup>a</sup>, O. Asunta<sup>a,b</sup>, and Tokamak Energy Ltd. Team<sup>a</sup>

<sup>a</sup>Tokamak Energy Ltd, 120A Olympic Avenue, Milton Park, Abingdon, OX14 4SA, UK

<sup>b</sup>Aalto University, Espoo, Finland

A new generation high field spherical tokamak, ST40, is currently under construction at Tokamak Energy Ltd. (TE). The main parameters of ST40 are:  $R_0=0.4-0.6\text{m}$ ,  $A=1.7-2.0$ ,  $I_{pl}=2\text{MA}$ ,  $B_t=3\text{T}$ ,  $\kappa=2.5$ . It will have power supplies based on ultracapacitors, liquid nitrogen cooled copper magnets, up to 2MW of neutral beam injected (NBI) power, and a pulse length of  $\sim 3\text{s}$  when operating at full power. To stabilize the highly elongated plasma, in addition to active vertical control, liquid nitrogen cooled passive plates will be installed. ST40 is aimed at demonstrating burning plasma condition parameters ( $nT\tau_E$ ) and may also be suitable for DT operations in future. The main physics and engineering challenges are caused by the high toroidal field, relatively high plasma current, and wall and divertor power loads.

Keywords: spherical tokamak, fusion, ultracapacitors

## 1. Introduction

Recent advances in the development of high temperature superconductors (HTS) [1], and encouraging results on a strong favorable dependence of electron transport on higher toroidal field (TF) in Spherical Tokamaks (ST) [4], open new prospects for a high field ST as a compact fusion reactor. The combination of the high  $\beta$ , the ratio of the plasma pressure to magnetic pressure  $p_{\text{plasma}}/p_{\text{mag}}=nk_B T/(B^2/2\mu_0)$ , which has been achieved in STs [5], and the high TF that can be produced by HTS TF magnets, could clear a path to lower-volume fusion devices, in accordance with the fusion power scaling proportional to  $\beta^2 B_t^4 V$ .

Until recently, STs have typically operated at toroidal magnetic fields around 0.3–0.5T. Recent upgrades to NSTX, Globus-M and MAST will bring them up to 1T fields. However, in order to reach high fusion performance in an ST, higher fields of 3–5T, or above, will be needed. Due to subsequent large forces and space limitations in a compact device, constructing an ST

operating at such fields will require innovative engineering solutions.

The long term plan of Tokamak Energy (TE) Ltd. is to build very high field STs using HTS magnets. As a first step, to develop and test solutions to some of the major engineering challenges, TE has designed ST40. It will use conventional copper magnets cooled to liquid nitrogen (LN2) temperatures and operate at fields up to 3T.

## 2. ST40 design

The overall structure of ST40 is depicted in Fig. 1. The main components are the inner and the outer vacuum chambers (Sec. 2.1.), and the toroidal and poloidal field coils (Sec. 2.2.). The outer vacuum chamber is supported by four legs and the entire assembly sits on top of the assembly platform (only partly visible in Fig. 1) that gives it enough elevation to allow access underneath the device.

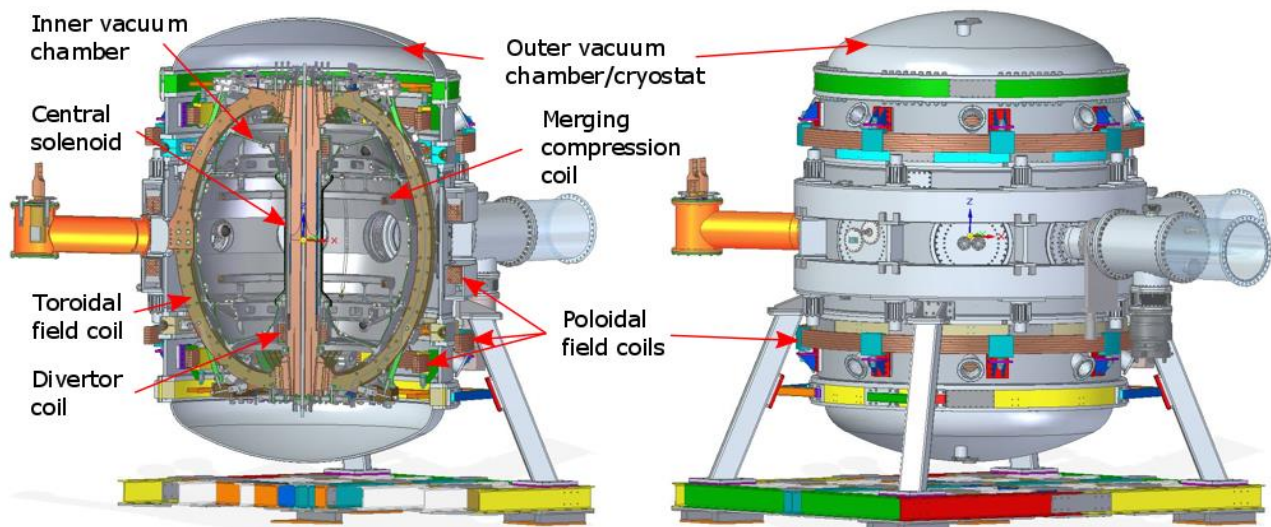


Fig. 1. Cutaway view (left) and outside view (right) of ST40 with the main components labelled.

## 2.1. Inner and outer vacuum chamber

ST40 will have a two-chamber vacuum system that consists of the inner vacuum chamber (IVC) and the outer vacuum chamber (OVC), illustrated in Fig. 1. The IVC is made of 10 mm thick stainless steel, apart from the centre tube (left panel of Fig. 2) that is made of 4 mm thick Inconel. On the high-field-side (HFS), the plasma will be limited by a set of eight fine grain graphite limiters (not yet installed in Fig. 2) that cover the entire height of the centre tube. On the low-field-side (LFS) the stainless steel of the IVC is the main plasma facing surface.

For plasma operations, the IVC (cf. right panel of Fig. 2) will be pumped down to  $\sim 10^{-8}$  mbar pressure. The vacuum within the OVC will be substantially lower, around  $10^{-4}$  mbar. The main purposes of the secondary vacuum are (i) to prevent icing of the TF magnets when they are cooled down to LN2 temperatures, and (ii) to work as an insulator between the IVC and the OVC, particularly during the baking of the IVC.



Fig. 2. Photos of the centre post of the device (left) and the entire ST40 inner vacuum chamber (right).

## 2.2. Coils

All the coils of ST40 are made of copper. It is a tried and tested magnet material with good structural strength and conductivity, particularly at liquid nitrogen temperatures.

The toroidal field magnet of ST40 consists of 24 turns arranged in 8 limbs of 3 turns each, all connected in series. The limbs are made of OFHC copper. All the turns are connected to the centre post with flexible demountable joints. The centre post itself consists of 24 copper (Cu-OF CW008A) wedges with a 15-degree twist in each to allow connecting one TF turn to the next. This design avoids the need for a TF compensating coil. The centre post with its 24 wedges is shown in the bottom panel of Fig. 3. The central solenoid, to be wound on the centre post, is not shown in the photo.

Another innovative solution is to use TF return limbs in the shape of constant tension curve. This design

minimizes the difference in the vertical expansion of the centre post and the return limbs over the permitted temperature rise during operations. Consequently, it helps minimize movement in the critical flexi-joints that connect the return limbs to the centre post wedges. One of the three turns of a TF return limb is shown in the top panel of Fig. 3.

On the LFS of the device, ST40 has three pairs of poloidal field (PF) coils (cf. Fig. 1), each positioned symmetrically relative to the midplane. Together with the divertor coils, located near the high-field-side top and bottom corners of the IVC, the PF coils are used for controlling the plasma current, position, and shape. Bar the TF coils, all the coils are made of Luvata OF-OK® copper. The PF coils and the divertor coil, like the TF coils, are designed to withstand 1 kV, whereas the maximum voltage for the solenoid coil is 1.2 kV.



Fig. 3. Photos of a copper TF return limb (top) and of the entire centre post with its 24 TF wedges (bottom).

Operating a small device with strong magnetic fields will result in large forces on the TF coils both in-plane ( $\mathbf{J} \times \mathbf{B}$  forces due to the interaction between current in the TF coil and the toroidal magnetic field) and out-of-plane ( $\mathbf{J} \times \mathbf{B}$  forces due to TF coil current and poloidal magnetic field from the PF coils). To accommodate these forces, ST40 has two large stainless steel rings on the OVC. Each the TF return limb is attached to both of these rings with two carbon fiber straps. In addition, there are two torque plates, one at the top and one at the bottom of the device, with eight carbon fiber straps each, to add extra support against twisting.

To obtain high toroidal field in the plasma, it is desired to use most of the centre post for TF coils. Thus, ST40 will only have a minimal central solenoid. Unlike in most conventional tokamaks, the solenoid is not used for inductive start-up. Instead, its purpose is to help maintain the flattop current and, thus, extend the length of the pulse.

For start-up, ST40 will use a process called merging compression [6] that was first developed for START [7]

and later utilized in MAST [8]. For that purpose, the design includes two in-vessel merging compression (MC) coils (recall Fig. 1) made of Luvata OF-OK® copper. In MC plasma start-up, the plasma is first formed as two rings around the two high voltage MC coils by rapidly ramping down the current in them. To allow a fast ramp, the MC coils are designed for maximum operating voltage of 6 kV. As the current in the coils vanishes, they are no longer able hold on to the plasma rings that at that point carry a significant amount of current. Due to the mutual attraction between the currents in the two rings, the rings then merge at the midplane. During the merging, reconnection of the magnetic fields of the two rings results in magnetic energy being converted into plasma thermal energy. This hot plasma is then compressed along the major radius using the PF coils.

All the coils are actively cooled, initially with water. Later on, liquid nitrogen can be used in all the coils except for the top two pairs of PF coils. This will enable extending the full power pulse length from ~1s to ~3s.

### 2.3. Power supplies

All ST40 power supplies incorporate capacitors for storing energy to enable their short, pulsed outputs. Merging compression power supply (PS) uses high voltage metallised polypropylene capacitors, while the power supplies for all the other coils utilize ultracapacitors due to their ability to store large amount of energy. Merging compression PS is a simple power supply: it has a thyristor single shot high voltage system with a diode freewheel. When the thyristor is triggered, the stored energy from the capacitors resonates with the coil to generate a damped sine wave current waveform.

The power supplies connected to the other coils are more sophisticated. Their output can be controlled during a pulse using a differential input signal. The power supply of the TF coils, with a maximum stored energy of 164 MJ, uses multiple parallel buck converters with Insulated Gate Bipolar Transistor (IGBT) switches to create a maximum 250kA output current for ~1.3s after a 1.7s ramp-up. Other PSs have H-Bridge inverters

and, hence, benefit from full 4-quadrant output capability. The stored energies of all the other PSs add up to roughly the same ~170 MJ as the TF PS.



Fig. 4. TF power supply charger (left) and part of the TF ultracapacitor banks (right).

### 2.4. Diagnostics

The diagnostic setup of ST40 consists of a wide array of diagnostics from machine monitoring (e.g. vacuum measurements, mass spectrometer, fast ion gauge, thermocouples, position monitoring, TF joint testing) to plasma diagnostics.

An extensive set of magnetic diagnostic, together with controllable power supplies (recall Sec. 2.3.), will allow current, position, and shape control during the pulse. Signals from the magnetic diagnostic will also be used for post-pulse equilibrium reconstruction. ST40 will have: two sets of poloidal magnetic field probes (34 probes per set), 19 flux loops, Rogowski coils (two for plasma current, one for each magnet, one for OVC, four for MC coil supports), 44 saddle coils, and two diamagnetic coils.

Several cameras will be installed on ST40. There are two visible light cameras: a fast camera with a frame rate of 10000fps (with the resolution of 256×256 pixels), and a high resolution camera with 90fps (2048×2048 pixels).

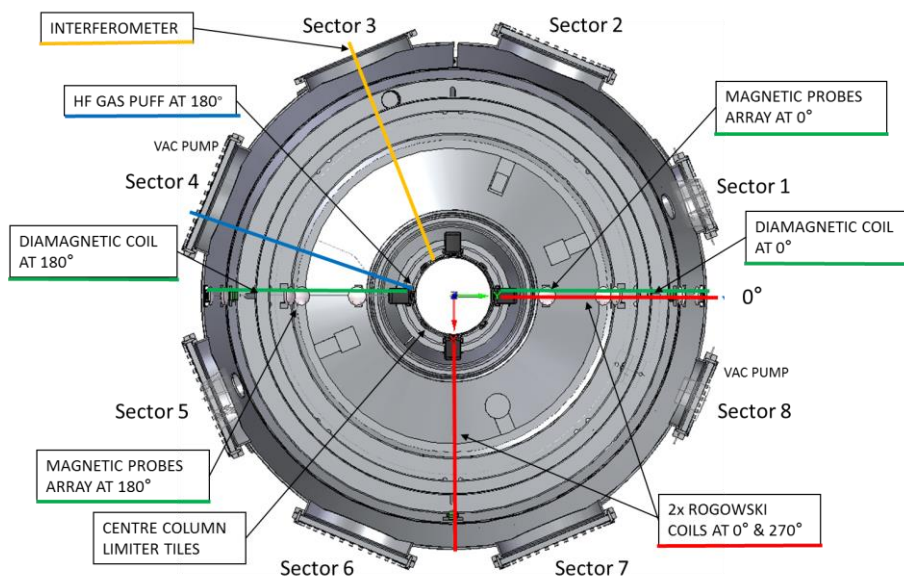


Fig. 5. Top-down view of ST40 indicating the locations of some of its diagnostics.

In addition, an infrared camera and a multifoil soft X-ray (SXR) camera system with three (3) cameras will be available. Every SXR camera will have four (4) diodes with different filters, each detecting the signals from the same 20 lines-of-sight. The viewing cones of the three cameras overlap and, hence, lend themselves for tomographic reconstruction.

Other diagnostics include a spectrometer with impurity Doppler measurements, 195 $\mu$ m interferometer with two lines-of-sight (one vertical and one horizontal), hard X-ray spectrometer, neutron spectrometer, NPA, ECE imaging, and ECE Doppler radiometer. The toroidal locations of some of the above-mentioned diagnostics are shown in Fig. 5.

### 2.5. Divertor

One of the challenges for compact fusion reactors are the potentially prohibitively high power loads on the divertor. In spherical tokamaks, operating in a double-null divertor (DND) configuration practically isolates the inner scrape-off-layer (SOL) from the outer scrape-off-layer. As particles and energy mostly escape the plasma from the HFS, most of the power loads are shared by the upper and lower outer divertor plates. This helps with the power loads because the outer divertor has more surface area than the inner divertor. It also has more space in which to implement advanced divertor configurations.

ST40 will operate in a DND configuration with graphite divertor tiles and cryo-pumping of the divertor region. The cryo-pumps will operate at about 4K, which will allow pumping also the hydrogenic species.

### 3. ST40 operational objectives

The goals of ST40 are (i) to demonstrate the feasibility of constructing and operating a high field ST, (ii) to show the benefits of a high field in an ST, and (iii) to achieve fusion relevant conditions, i.e., a high  $nT\tau_E$ .

As mentioned earlier, ST40 will use the merging compression plasma formation method. Empirical scaling, based on experimental data from existing devices predicts that the plasma temperature resulting from merging compression is proportional to the square of the merging poloidal magnetic field [9],[10]. In ST40, this field will be at least three times higher than in MAST, which demonstrated electron and ion temperatures up to 1.2keV. Therefore, the expectation of multi-keV temperatures is justified. Moderate extrapolation of the achievable plasma current from MAST and START data predicts achievement of 2MA in ST40 with the support from the central solenoid and the current driven by neutral beam injection (NBI). As the ST40 operating regime assumes densities in 1–5 $\cdot 10^{20}$ m<sup>-3</sup> range, conditions close to burning plasma requirements ( $nT\tau_E > 3\cdot 10^{21}$ ) are expected, providing that the plasma confinement will follow optimistic predictions based on MAST and NSTX data.

### 4. Summary

Tokamak Energy Ltd. is currently constructing ST40, a spherical tokamak with  $R_0=0.4\text{--}0.6$ m,  $A=1.7\text{--}2.0$ ,  $I_p=2$ MA,  $B_t=3$ T,  $\kappa=2.5$ . Active vertical control will be used, and liquid nitrogen cooled passive plates will be installed to stabilize the highly elongated plasma. The device will be furnished with up to two 40keV, 1MW neutral beam injectors, and could be suitable for DT operations in future. The pulse length in the first stage with water-cooled magnets will be  $\sim 1$ s of full power operation but, later on when using LN2 cooling, that can be increased up to  $\sim 3$ s. The ultimate goal of ST40 is to demonstrate burning plasma condition parameters ( $nT\tau_E$ ). It will also be used to develop and test solutions to some of the major engineering challenges in constructing compact high field spherical tokamaks.

### Acknowledgments

The members of the Tokamak Energy Ltd. Team who provided the images for this publication are thankfully acknowledged: P. Tigwell (Fig. 1), G. Dunbar (Figs. 2 and 3), A. McFarland (Fig. 4), and G. Whitfield (Fig. 5).

### References

- [1] M. Gryaznevich et al., Progress in application of high temperature superconductor in tokamak magnets, *Fusion Engineering and Design* 88 (2013) 1593
- [2] W. Fietz et al., Prospects of High Temperature Superconductors for fusion magnets and power applications, *Fusion Engineering and Design*, 88 (2013) 440-445
- [3] W. Fietz et al., High-Current HTS Cables: Status and Actual Development, *IEEE Transactions on Applied Superconductivity*, 26 (2016) 4800705
- [4] M. Valovic et al., Scaling of H-mode energy confinement with  $I_p$  and  $BT$  in the MAST spherical tokamak, *Nuclear Fusion* 49 (2009) 075016
- [5] A. Sykes, High  $\beta$  produced by neutral beam injection in the START (Small Tight Aspect Ratio Tokamak) spherical tokamak, *Physics of Plasmas* 4 (1997) 1665
- [6] P. Buxton et al., Merging Compression start-up in ST40, P1.047, 29th Symposium on Fusion Technology (SOFT 2016)
- [7] A. Sykes et al., First results from the START experiment, *Nuclear Fusion* 32 (4) (1992) 694.
- [8] A. Sykes et al., First results from MAST, *Nuclear Fusion* 41 (2001) 1423
- [9] Y. Ono et al., High power heating of magnetic reconnection in merging tokamak experiments, *Physics of Plasmas* 22 (2015) 055708
- [10] M. Gryaznevich and A. Sykes, Merging-compression formation of high temperature tokamak plasma, Submitted to *Nuclear Fusion* "Special issue of papers arising from ICCP 2016"